

Synchrotron-based X-ray Fluorescence Microscopy in Conjunction with Nanoindentation to Study Molecular-Scale Interactions of Phenol–Formaldehyde in Wood Cell Walls

Joseph E. Jakes,^{*,†} Christopher G. Hunt,[†] Daniel J. Yelle,[†] Linda Lorenz,[†] Kolby Hirth,[‡] Sophie-Charlotte Gleber,[§] Stefan Vogt,[§] Warren Grigsby,^{||} and Charles R. Frihart[†]

[†]Forest Biopolymers Science and Engineering, Forest Products Laboratory, U.S. Forest Service, One Gifford Pinchot Drive, Madison, Wisconsin 53726, United States

[‡]Analytical Chemistry and Microscopy, Forest Products Laboratory, U.S. Forest Service, One Gifford Pinchot Drive, Madison, Wisconsin 53726, United States

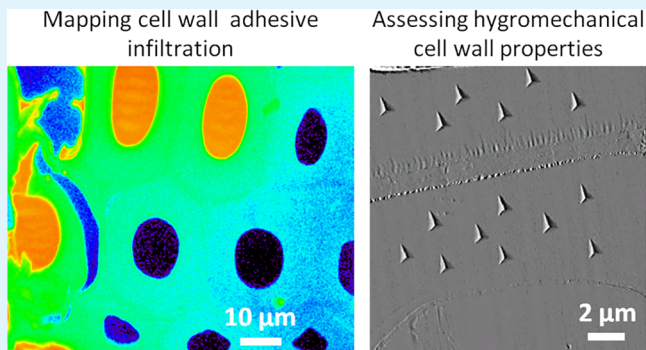
[§]X-ray Science Division, Argonne National Laboratory, 9700 S. Cass Avenue, Argonne, Illinois 60439, United States

^{||}Scion, 49 Sala Street, Rotorua 3010, New Zealand

Supporting Information

ABSTRACT: Understanding and controlling molecular-scale interactions between adhesives and wood polymers are critical to accelerate the development of improved adhesives for advanced wood-based materials. The submicrometer resolution of synchrotron-based X-ray fluorescence microscopy (XFM) was found capable of mapping and quantifying infiltration of Br-labeled phenol–formaldehyde (BrPF) into wood cell walls. Cell wall infiltration of five BrPF adhesives with different average molecular weights (MWs) was mapped. Nanoindentation on the same cell walls was performed to assess the effects of BrPF infiltration on cell wall hygromechanical properties. For the same amount of weight uptake, lower MW BrPF adhesives were found to be more effective at decreasing moisture-induced mechanical softening. This greater effectiveness of lower MW phenolic adhesives likely resulted from their ability to more intimately associate with water sorption sites in the wood polymers. Evidence also suggests that a BrPF interpenetrating polymer network (IPN) formed within the wood polymers, which might also decrease moisture sorption by mechanically restraining wood polymers during swelling.

KEYWORDS: X-ray fluorescence microscopy, nanoindentation, wood, adhesive, infiltration



INTRODUCTION

Wood has been used as a structural material for millennia because of its regular availability and exceptional specific strength. Even today, wood and wood-based composites (including plywood, fiberboard, and laminated veneer lumber) continue to be the most cost-effective construction materials of choice. New advanced timber products, such as cross-laminated timber, are also under development and becoming viable substitutes for steel and concrete in larger structures, such as midrise buildings and bridges.^{1,2} From an environmental perspective, wood-based products are attractive because wood can be sustainably sourced, and wood-based products have a lower embodied energy and are responsible for less air and water pollution than concrete and steel.^{3,4} However, an integral component of most advanced forest products is the adhesive and the wood–adhesive bondline. One durability and performance issue is the susceptibility of wood–adhesive bondlines to failures caused by moisture-induced swelling of wood near

bondlines.⁵ Unfortunately, researchers are hindered by lack of understanding of molecular-level interactions between adhesives and wood that lead to moisture durability.

Wood is an anisotropic, cellular material with numerous levels of structure, ranging from component polymers to tree stem.^{6,7} Typical secondary cell walls are nanofiber-reinforced composites of highly oriented, semicrystalline cellulose microfibrils embedded in an organized matrix of hemicelluloses and lignin.^{8,9} From a solubility parameter viewpoint, lignin and cellulose are incompatible, but the molecular-level architecture of wood may overcome this by using hemicelluloses to bridge between the cellulose microfibrils and lignin.¹⁰ Another important component of wood is water, which absorbs at the accessible hydroxyl and other polar chemical groups in

Received: December 12, 2014

Accepted: March 10, 2015

Published: March 10, 2015

amorphous cellulose, hemicelluloses, and lignin. The amount of absorbed water, which is directly related to the extent of swelling, depends on ambient temperature and relative humidity (RH) and is driven by complex thermodynamic processes that are poorly understood.¹¹ Typical room-temperature absorption and desorption curves have sigmoid shapes with an absorption–desorption hysteresis. For moisture contents typically up to 30–40%, called fiber saturation point, water in wood is bound at sorption sites within the wood polymers.^{11–14} At higher moisture levels, the amount of bound water remains constant and free water forms in wood cavities. Because moisture-induced swelling is caused by changes in the amount of bound water, a research focus interest is to understand how to control the amount of bound water.

Although some moisture-durable wood adhesives are available, they have been developed over decades from empirical testing. An improved mechanistic understanding of what leads to their moisture durability would accelerate the improvement of current wood adhesives and development of new wood adhesives. Phenol–formaldehyde (PF) is one of the most moisture-durable wood adhesives available,⁵ and PF treatments of bulk wood have also long been known to improve moisture-related dimensional stability of wood.¹⁵ Although the general consensus is that infiltration of PF into the polymer structure of wood cell walls is responsible for this dimensional stability,^{5,15–17} the underlying molecular-scale mechanisms are still debated. For example, it has not been determined conclusively if PF forms covalent bonds with wood polymers, although the potential has been proposed.¹⁸ Molecular weight (MW) and molecular weight distribution of the PF seem to play a role. In bulk wood treatments, higher weight uptake and greater dimensional stability are achieved when PF treatments with lower MW are used.^{15,19,20} A recent study that utilized solid-state NMR and dynamic mechanical analysis showed that low-MW PF can be miscible with matrix wood polymers at the molecular-scale, whereas a PF distribution that is a predominately higher MW with only a small amount of low-MW PF cannot and leads to a phase-separated system that causes overall plasticization of the lignin, as evidenced by decreased lignin glass transition temperature.²¹ What is not clear is whether dimensional stability is achieved solely by cell wall bulking, as indicated by higher weight uptake, or if molecular-scale interactions with wood polymers may also be a factor.

In this study, Br-labeled phenol–formaldehyde (BrPF) adhesives with five different degrees of polymerization are used to make wood–adhesive bondlines. Then, the high spatial resolution and sensitivity of synchrotron-based X-ray fluorescence microscopy (XFM) are applied to quantify the amount of Br, and therefore BrPF, that infiltrated into individual wood cell walls. Finally, nanoindentation under dry air and 78% relative humidity (RH) on the same cell walls is used to directly compare the amount of BrPF infiltration to changes in hygromechanical cell wall properties. Cell wall mechanical properties are highly moisture sensitive,^{22,23} and changes in hygromechanical properties will be used to gain insights into how BrPF infiltration modifies moisture-dependent cell wall properties.

MATERIALS AND METHODS

Full experimental details of the bromine-labeled phenol–formaldehyde (BrPF) adhesive and bondlines are given in the Supporting Information. Briefly, BrPF adhesive was prepared by replacing phenol with 3-bromophenol in the adhesive formula on an equal molar basis.

After the initial methylation step, condensation stage commenced and aliquots were removed after 45, 85, 115, 135, and 155 min. Gel permeation chromatography (GPC) qualitatively showed a steady growth in high-MW components with increasing condensation time. Wood–adhesive bondlines were prepared for each condensation time using pristine tangential–longitudinal surfaces in latewood loblolly pine (*Pinus taeda*). Ancillary experiments performed to determine whether Br could detach from the BrPF are also described in the Supporting Information. Approximately 1% of the Br atoms may have detached and formed free Br ions under the bonding conditions.

X-ray fluorescence microscopy (XFM) of 2 μm -thick transverse sections of wood–BrPF bondlines was performed at beamline 2-ID-E at the Advanced Photon Source (APS) at Argonne National Laboratory (Argonne, Illinois, USA). For each BrPF condensation time, one section was prepared and imaged. The sections were oriented in the beamline sample holder to minimize interface smearing effects in the tangential-side cell walls (Figure S1 in the Supporting Information). The beam had an incident energy of 15.0 keV and was focused with a 10 cm zone plate to a spot size of 0.28 by 0.28 μm full width at half-maximum. Images were built up using 0.15 μm steps with 20 ms dwell times. Data analysis was carried out using the MAPS software package.²⁴ Full XFM experimental details are given in the Supporting Information.

Rows of daughter cells that included BrPF-infiltrated and control cell walls were chosen from the XFM images for nanoindentation. Nanoindents were placed in the tangential side of the S2 secondary cell wall layers of the chosen cells in the blocks from which the 2 μm -thick XFM sections were cut. A Hysitron (Minneapolis, Minnesota, USA) TriboIndenter equipped with a Berkovich probe was used. Multiloading indents and the structural compliance method^{25,26} were employed to remove artifacts caused by edge effects and specimen-scale flexing before calculating the nanoindentation elastic modulus (E_s^{NI}) and Meyer's hardness (H). Relative humidity (RH) inside the nanoindentation enclosure was controlled with an InstruQuest (Coconut Creek, Florida, USA) HumiSys HF RH generator. Specimens were conditioned inside the enclosure at 78% RH for 2 days, and the RH was maintained during experiments. Then, fresh nanoindentation surfaces were prepared on each specimen and they were conditioned under dry air for 2 days inside the enclosure before experiments were performed on the same cell walls that had been also tested at 78% RH. Full nanoindentation experimental details and analyses are given in the Supporting Information.

RESULTS AND DISCUSSION

The XFM Br signal was used to map and quantify BrPF penetration into wood. XFM maps of 85 min and 155 min BrPF samples are shown in Figure 1a,b, respectively. Highest Br concentrations were visually evident in the solid adhesive in the bondline and within a few lumina filled with adhesive. Moreover, the lower average MW BrPF (85 min) sample filled more lumina many cells from the bondline compared to the 155 min BrPF sample. Presumably, the 85 min BrPF traveled to these lumina through rays cells and pits, as has been observed with three-dimensional X-ray computed tomography.^{27,28} The higher MW 155 min BrPF sample did not flow as deeply into the wood substrate.

The Br concentration measured within the wood cell wall quantified the amount of adhesive infiltration and is later in this paper compared to cell wall mechanical properties assessed using nanoindentation. Because all phenol units in the BrPF were tagged with Br, the concentration of Br in each BrPF polymer chain should be independent of MW. Also, because Br was covalently bound to the adhesive polymer, there was more certainty that the Br marker was an accurate representative of the adhesive concentration, as opposed to Na and Rb ionic tags that have been shown to diffuse and separate from the adhesive.²⁷ Despite this, a small, but detectable, Br concen-

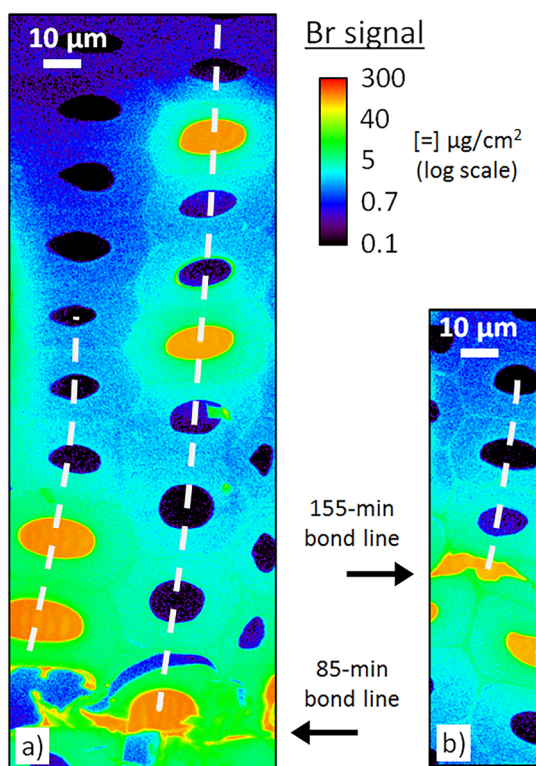


Figure 1. X-ray fluorescence microscopy (XFM) Br maps of transverse sections from (a) 85 min BrPF sample (left) and (b) 155 min sample (right) bondlines. Dashed lines indicate rows of daughter cells chosen for nanoindentation experiments; arrows indicate bondlines.

tration was observed in cell walls far from the bondline or BrPF-filled lumina. In a control experiment, no Br could be detected in unmodified wood cell walls, suggesting the Br present far from adhesive bondlines was not naturally occurring. We cannot be certain if these small amounts of Br resulted from adhesive infiltration during the bonding process, diffusion of Br ions that separated from the BrPF through wood cell walls during curing, diffusion of Br ions in the water during section preparation, or some combination. Although this Br background was undesirable, it was much lower than the Br signal in cell walls near the solid BrPF (bondline). The background Br signals varied between 1 and 2 $\mu\text{g}/\text{cm}^2$ for each section, and accordingly we designate cells with Br signal $<2 \mu\text{g}/\text{cm}^2$ to be control cells.

Infiltration of BrPF into wood cell walls has previously been shown using energy dispersive X-ray (EDX) techniques.^{19,29} In contrast to this electron-based technique, XFM has multiple orders of magnitude higher sensitivity because X-rays do not produce Bremsstrahlung background.³⁰ In the XFM maps (Figure 1), gradients of BrPF infiltration were observed through the wood cell walls, with amount of BrPF infiltration decreasing with increasing distance from the BrPF–cell wall interface. Furthermore, for a given cell wall, amount of adhesive infiltration appeared to depend only on distance from the BrPF–cell wall interface, meaning that lines equidistant from the interface and middle lamellae have approximately the same level of BrPF infiltration.

Lines of two to four nanoindentations equidistant from the lumen surface and middle lamella were placed in the tangential sides of the S2 secondary cell walls (Figure 2) in the rows of daughter cells chosen from XFM Br maps (Figure 1a,b for the 85 and

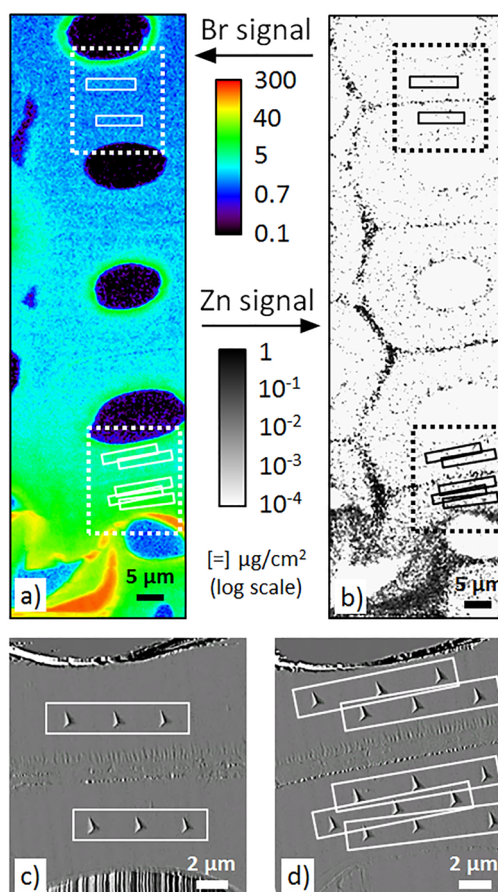


Figure 2. X-ray fluorescence microscopy (XFM) for (a) Br (top, left) and (b) Zn maps (top, right) from the 45 min BrPF sample bondline. The top dashed box in panels a and b corresponds to the atomic force microscope (AFM) image in panel c; the bottom dashed box corresponds to the AFM image in panel d. AFM images show nanoindentations placed in cell walls in the wood block from which the XFM section was cut. Solid rectangular boxes define different regions of interest (ROIs).

155 min sections, respectively). Multiple lines of nanoindentations were performed in cell walls with large gradients of infiltration to capture multiple levels of infiltration (Figure 2d). Regions of interest (ROIs) were defined for each nanoindent line (Figure 2) and the average mechanical property for each ROI matched to the average Br signal from the ROI in the Br XFM map. Maps of zinc (Figure 2b), a naturally occurring element that has a higher concentration in the middle lamella,³¹ were also found useful for positioning the ROIs.

Meyer hardness (H) and nanoindentation elastic modulus (E_s^{NI}) for each BrPF condensation level are shown in Figures 3 and 4, respectively. For the chosen daughter cell rows, lower MW adhesives (45, 85, and 115 min) resulted in cell walls with higher amounts of infiltration than higher MW adhesives (135 and 155 min), consistent with previous studies where bulk PF treatments with lower MW distributions resulted in higher weight uptakes.^{15,19,20} For H , the general trend was an increase in H values with an increase in Br signal under both dry and 78% RH conditions. The H assesses the plasticity of the cell walls and is primarily influenced by the matrix properties in the secondary cell wall.^{9,32} Increasing H with infiltration under dry conditions indicated the infiltrated BrPF reinforced the cell wall matrix and did not plasticize it, as observed previously using a

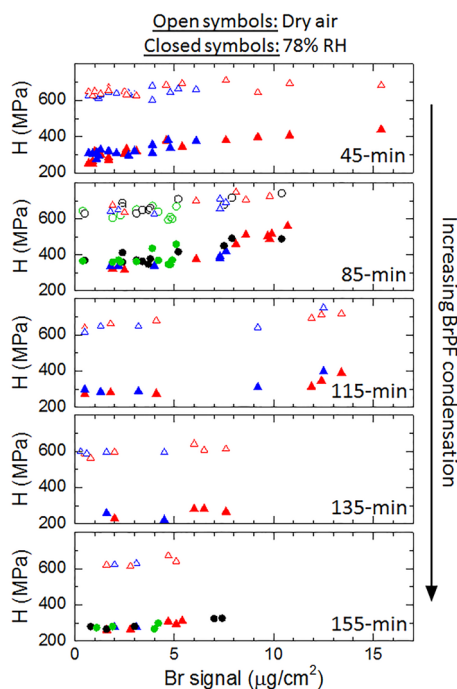


Figure 3. Hardness H of S2 secondary cell wall layers as a function of BrPF infiltration, humidity conditioning (open symbols are dry air, closed symbols are 78% RH), and increasing level of BrPF condensation. Each symbol shape (circle or triangle) represents a different row of daughter cells, and different colors within a symbol shape distinguish the two sides of the double cell wall.

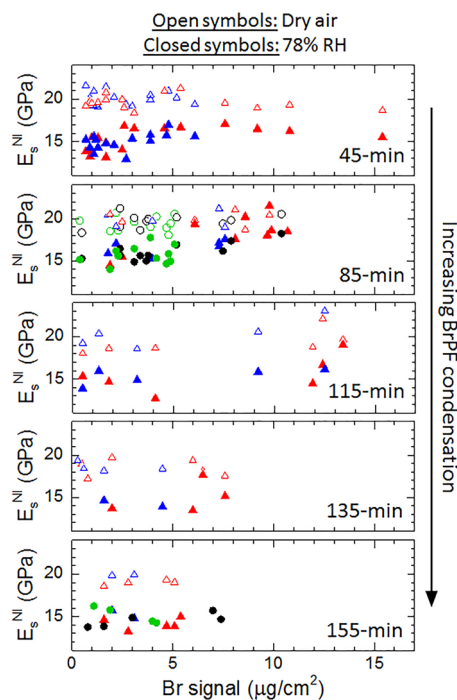


Figure 4. Nanoindentation elastic modulus E_s^{NI} of S2 secondary cell wall layers as a function of BrPF infiltration, humidity conditioning (open symbols are dry air, closed symbols are 78% RH), and BrPF condensation. Each symbol shape (circle or triangle) represents a different row of daughter cells, and different colors within a symbol shape distinguish the two sides of the double cell wall.

high-MW PF with a small low-MW fraction²¹ or in uncured PF treatments.³³ At 78% RH it was also found that E_s^{NI} increased with Br signal (closed symbols in Figure 4). However, under dry air, little, if any, effect of BrPF infiltration on E_s^{NI} was observed. In the longitudinal orientation, E_s^{NI} is controlled primarily by orientation of the stiff cellulose microfibrils,³⁴ although mechanical softening of the matrix still causes some decrease in longitudinal elastic modulus.³⁵ The BrPF reinforcement of the matrix observed in the dry air H was likely counteracted by swelling of the matrix by the BrPF infiltration, and therefore led to larger spacing between cellulose microfibrils, which has previously been shown to decrease E_s^{NI} .^{32,34} The larger effect of BrPF infiltration at 78% RH on the E_s^{NI} suggests that infiltration is preventing some moisture sorption along with its associated mechanical softening of the cell wall matrix. This overall trend of a substantial increase in H and relatively small increase in E_s^{NI} is consistent with previous work of nanoindentation of PF-infiltrated wood cell walls near wood–adhesive bondlines.^{36,37}

Both H and E_s^{NI} decreased at 78% RH compared to dry air conditioning because the absorbed moisture has the effect of plasticizing the cell wall matrix polymers. To better compare the effect of BrPF infiltration on moisture-induced mechanical softening, the percentage decreases of H and E_s^{NI} were calculated for all ROIs with both dry air and 78% RH nanoindentation results (Figure 5). For control cells (Br signal

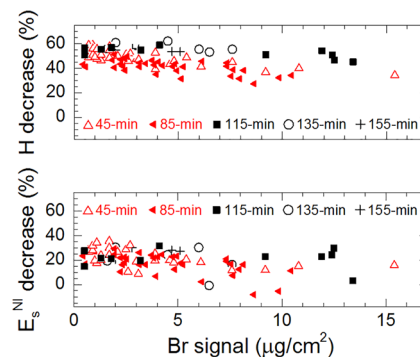


Figure 5. Percentage decreases in hardness H and nanoindentation elastic modulus E_s^{NI} as functions of BrPF infiltration. Percentage decrease was defined as the change in property from dry air to 78% RH divided by the property under dry air multiplied by 100.

$<2 \mu\text{g}/\text{cm}^2$), average decrease in H (53%) was greater than the E_s^{NI} decrease (25%), which is similar to previous nanoindentation results in the longitudinal direction of unmodified wood cell walls conditioned at low and high RH.^{22,23} For BrPF-infiltrated cell walls, the H decrease remained larger than the E_s^{NI} decrease for all amounts of infiltration. The larger difference in H indicated that H is more sensitive to changes in cell wall matrix properties than E_s^{NI} . For E_s^{NI} , the percentage decrease approached 0 at higher BrPF infiltration and no differences in adhesive condensation time (MW) were observed.

In H , a MW effect was observed, with the low level condensation 45 and 85 min samples showing a smaller percentage decrease for a given amount of BrPF infiltration than the higher condensation 115, 135, and 155 min BrPF samples. This suggests that lower MW adhesives were more efficient in modifying cell walls to prevent moisture sorption and therefore improving dimensional stability. Furthermore, the

mechanism for moisture durability must be more than solely an adhesive weight uptake effect.

At the molecular-scale, the lower MW BrPF that infiltrated into wood cell walls was likely more miscible with the wood polymers than the higher MW BrPF. The more miscible BrPF could have occupied more of the water sorption sites (e.g., hydroxyl and polar chemical groups) in the amorphous wood polymers. With fewer sorption sites, the thermodynamics of water sorption would change and the equilibrium moisture content for a given RH would decrease, as observed by the decrease in moisture-induced plasticization (Figure 5). Arguably, the infiltration of the lower MW BrPF and curing creates an interpenetrating polymer network (IPN), as has been previously proposed,²¹ because the increase in H even under dry conditions suggests that cell wall matrix polymers have been reinforced (Figure 3). However, whether the contribution of an IPN toward moisture durability is to only block sorption sites, or if this IPN also provides mechanical constraint at the nanoscale to prevent swelling, is uncertain.

This work provides new insights into how to design a moisture durable wood adhesive. Nearn originally claimed that the moisture durability of PF bondlines in wood was directly dependent on PF infiltrating the cell wall.³⁸ However, in practice simply using a low MW PF to infiltrate the cell wall is not feasible because it will over-penetrate wood and lead to an undesirable starved bondline. Some viscous high MW PF is needed to remain in the bondline and fill the gap. Our current work indicates that of the PF that can infiltrate the cell wall only the lower MW components contribute toward minimizing the uptake of water that leads to swelling by either occupying water sorption sites in wood polymers or forming an IPN. The higher MW portion of the PF MW range that can infiltrate the cell walls does not contribute to minimizing the uptake of water and may even be detrimental because it occupies space and prevents some of beneficial lower MW PF from infiltrating the wood cell wall. Therefore, an effective strategy might be to have a bimodal PF MW distribution that only includes this beneficial low MW PF fraction and a high MW gap-filling fraction.

CONCLUSION

Synchrotron-based XFM was used to accurately map BrPF infiltration into wood cell walls, and nanoindentation was used to assess the effects of infiltration on cell wall hygromechanical properties. Five different BrPF MWs were studied. Nanoindentation results showed that BrPF reinforced the cell wall matrix and that lower MW BrPF samples were more effective in preventing moisture-induced softening of the cell wall matrix for a given percentage weight uptake of adhesive. The formation of an interpenetrating polymer network by the low-MW BrPF was supported.

ASSOCIATED CONTENT

Supporting Information

Further details describing BrPF formulation, BrPF characterization, XFM protocols, nanoindentation protocols, and nanoindentation analyses. This material is available free of charge via the Internet at <http://pubs.acs.org>.

AUTHOR INFORMATION

Corresponding Author

*J. E. Jakes. E-mail: jjakes@fs.fed.us.

Notes

The authors declare no competing financial interest.

ACKNOWLEDGMENTS

The use of Advanced Photon Source facilities was supported by the U.S. Department of Energy, Basic Energy Sciences, Office of Science, under contract number W-31-109-Eng-38. Partial funding was provided by the FHA Cooperative Research Program for Covered Timber Bridges. J.E.J. acknowledges funding from 2011 USDA Forest Service PECASE Award.

REFERENCES

- (1) Lehmann, S. Low Carbon Construction Systems Using Prefabricated Engineered Solid Wood Panels for Urban Infill to Significantly Reduce Greenhouse Gas Emissions. *Sustainable Cities Soc.* **2013**, *6*, 57–67.
- (2) Robertson, A. B.; Lame, F. C. F.; Cole, R. J. A Comparative Cradle-to-Gate Life Cycle Assessment of Mid-Rise Office Building Construction Alternatives: Laminated Timber or Reinforced Concrete. *Buildings* **2012**, *2*, 245–270.
- (3) Lippke, B.; Wilson, J.; Perez-Garcia, J.; Bowyer, J.; Meil, J. CORRIM: Life-Cycle Environmental Performance of Renewable Building Materials. *For. Prod. J.* **2004**, *54*, 8–19.
- (4) Oliver, C. D.; Nassar, N. T.; Lippke, B. R.; McCarter, J. B. Carbon, Fossil Fuel, and Biodiversity Mitigation with Wood and Forests. *J. Sustainable For.* **2014**, *33*, 248–275.
- (5) Frihart, C. R. Adhesive Groups and How They Relate to the Durability of Bonded Wood. *J. Adhes. Sci. Technol.* **2009**, *23*, 611–627.
- (6) Wiedenhoef, A. C. Structure and Function of Wood. In *Handbook of Wood Chemistry and Wood Composites*; Rowell, R. M., Ed.; CRC Press: Boca Raton, FL, 2013; pp 9–32.
- (7) Rowell, R. M.; Petterson, R.; Tshabalala, M. A. Cell Wall Chemistry. In *Handbook of Wood Chemistry and Wood Composites*; Rowell, R. M., Ed.; CRC Press: Boca Raton, FL, 2013; pp 33–72.
- (8) Terashima, N.; Kitano, K.; Kojima, M.; Yoshida, M.; Yamamoto, H.; Westermark, U. Nanostructural Assembly of Cellulose, Hemicellulose, and Lignin in the Middle Layer of Secondary Wall of Ginkgo Tracheid. *J. Wood Sci.* **2009**, *55*, 409–416.
- (9) Salmen, L.; Burgert, I. Cell Wall Features with Regard to Mechanical Performance. A Review. COST Action E35 2004–2008: Wood Machining - Micromechanics and Fracture. *Holzforschung* **2009**, *63*, 121–129.
- (10) Hansen, C. M.; Bjorkman, A. Ultrastructure of Wood from a Solubility Parameter Point of View. *Holzforschung* **1998**, *52*, 335–344.
- (11) Englund, E.; Thygesen, L. A Critical Discussion of the Physics of Wood–Water Interactions. *Wood Sci. Technol.* **2013**, *47*, 141–161.
- (12) Berry, S. L.; Roderick, M. L. Plant-Water Relations and the Fibre Saturation Point. *New Phytol.* **2005**, *168*, 25–37.
- (13) Stamm, A. Review of Nine Methods for Determining the Fiber Saturation Points of Wood and Wood Products. *Wood Sci.* **1971**, *4*, 114–128.
- (14) Hernández, R.; Bizoñ, M. Changes in Shrinkage and Tangential Compression Strength of Sugar Maple below and above the Fiber Saturation Point. *Wood Fiber Sci.* **1994**, *26*, 360–369.
- (15) Stamm, A. J.; Seborg, R. M. Minimizing Wood Shrinkage and Swelling. *Ind. Eng. Chem.* **1936**, *28*, 1164–1169.
- (16) Kamke, F. A.; Lee, J. N. Adhesive Penetration in Wood—A Review. *Wood Fiber Sci.* **2007**, *39*, 205–220.
- (17) Nearn, W. Wood-Adhesive Interface Relations. *Off. Dig., Fed. Soc. Paint Technol.* **1965**, *37*, 720–733.
- (18) Pizzi, A.; Mtsweni, B.; Parsons, W. Wood-Induced Catalytic Activation of PF Adhesives Autopolymerization vs. PF/Wood Covalent Bonding. *J. Appl. Polym. Sci.* **1994**, *52*, 1847–1856.
- (19) Furuno, T.; Imamura, Y.; Kajita, H. The Modification of Wood by Treatment with Low Molecular Weight Phenol-Formaldehyde Resin: A Properties Enhancement with Neutralized Phenolic-Resin and Resin Penetration into Wood Cell Walls. *Wood Sci. Technol.* **2004**, *37*, 349–361.

- (20) Gabrielli, C. P.; Kamke, F. A. Phenol–Formaldehyde Impregnation of Densified Wood for Improved Dimensional Stability. *Wood Sci. Technol.* **2009**, *44*, 95–104.
- (21) Laborie, M.-P. G.; Salmen, L.; Frazier, C. E. A Morphological Study of the Wood/Phenol-Formaldehyde Adhesive Interphase. *J. Adhes. Sci. Technol.* **2006**, *20*, 729–741.
- (22) Yu, Y.; Fei, B.; Wang, H.; Tian, G. Longitudinal Mechanical Properties of Cell Wall of Masson Pine (*Pinus massoniana* Lamb) as Related to Moisture Content: A Nanoindentation Study. *Holzforschung* **2010**, *65*, 121–126.
- (23) Bertineti, L.; Hangen, U. D.; Eder, M.; Leibner, P.; Fratzl, P.; Zlotnikov, I. Characterizing Moisture-Dependent Mechanical Properties of Organic Materials: Humidity-Controlled Static and Dynamic Nanoindentation of Wood Cell Walls. *Philos. Mag.* **2014**, 1–7.
- (24) Vogt, S. MAPS: A Set of Software Tools for Analysis and Visualization of 3D X-ray Fluorescence Data Sets. *J. Phys. IV* **2003**, *104*, 635–638.
- (25) Jakes, J. E.; Frihart, C. R.; Beecher, J. F.; Moon, R. J.; Stone, D. S. Experimental Method to Account for Structural Compliance in Nanoindentation Measurements. *J. Mater. Res.* **2008**, *23*, 1113–1127.
- (26) Jakes, J. E.; Frihart, C. R.; Beecher, J. F.; Moon, R. J.; Resto, P. J.; Melgarejo, Z. H.; Surez, O. M.; Baumgart, H.; Elmustafa, A. A.; Stone, D. S. Nanoindentation near the Edge. *J. Mater. Res.* **2009**, *24*, 1016–1031.
- (27) Paris, J. L.; Kamke, F. A.; Mbachu, R.; Gibson, S. K. Phenol Formaldehyde Adhesives Formulated for Advanced X-ray Imaging in Wood-Composite Bondlines. *J. Mater. Sci.* **2013**, *49*, 580–591.
- (28) Hass, P.; Wittel, F. K.; Mendoza, M.; Herrmann, H. J.; Niemz, P. Adhesive Penetration in Beech Wood: Experiments. *Wood Sci. Technol.* **2011**, *46*, 243–256.
- (29) Smith, L. A.; Cote, W. A. Studies of Penetration of Phenol-Formaldehyde Resin into Wood Cell Walls with the SEM and Energy-Dispersive X-ray Analyzer. *Wood Fiber Sci.* **1971**, *3*, 56–57.
- (30) Paunesku, T.; Vogt, S.; Maser, J.; Lai, B.; Woloschak, G. X-ray Fluorescence Microprobe Imaging in Biology and Medicine. *J. Cell. Biochem.* **2006**, *99*, 1489–1502.
- (31) Saka, S.; Goring, D. The Distribution of Inorganic Constituents in Black Spruce Wood As Determined by TEM-EDXA. *J. Jpn. Wood Res. Soc.* **1983**, *29*, 648–656.
- (32) Gindl, W.; Gupta, H. S.; Schoberl, T.; Lichtenegger, H. C.; Fratzl, P. Mechanical Properties of Spruce Wood Cell Walls by Nanoindentation. *Appl. Phys. A: Mater. Sci. Process.* **2004**, *A79*, 2069–2073.
- (33) Shams, M. I.; Yano, H. Compressive Deformation of Phenol Formaldehyde (PF) Resin-Impregnated Wood Related to the Molecular Weight of Resin. *Wood Sci. Technol.* **2010**, *45*, 73–81.
- (34) Jäger, A.; Bader, T.; Hofstetter, K.; Eberhardsteiner, J. The Relation between Indentation Modulus, Microfibril Angle, and Elastic Properties of Wood Cell Walls. *Composites, Part A* **2011**, *42*, 677–685.
- (35) Salmén, L. Micromechanical Understanding of the Cell-Wall Structure. *C. R. Biol.* **2004**, *327*, 873–880.
- (36) Gindl, W.; Schoberl, T.; Jeronimidis, G. The Interphase in Phenol-Formaldehyde and Polymeric methylene Di-Phenyl-Di-Isocyanate Glue Lines in Wood. *Int. J. Adhes. Adhes.* **2004**, *24*, 279–286.
- (37) Hunt, C. E.; Jakes, J. E.; Grigsby, W. Evaluation of Adhesive Penetration of Wood Fibre by Nanoindentation and Microscopy. In *BIOCOMP 2010: 10th Pacific Rim Bio-based Composites Symposium*, Banff, Canada, October 5–8, 2010; pp 216–226.
- (38) Nearn, W. T. Application of the Ultrastructure Concept in Industrial Wood Products Research. *Wood Sci.* **1974**, *6*, 285–293.